

# Biomimetic Nanocarrier for Direct Cytosolic Drug Delivery\*\*

Zhihong Zhang, Weiguo Cao, Honglin Jin, Jonathan F. Lovell, Mi Yang, Lili Ding, Juan Chen, Ian Corbin, Qingming Luo, and Gang Zheng\*

Dedicated to Professor Britton Chance on the occasion of his 96th birthday

The ability to transport a large quantity of drug molecules into cytosolic compartments of cancer cells has powerful implications in modern molecular therapeutics because the sites of action of the drugs are often cytosolic organelles.<sup>[1–4]</sup> Furthermore, direct cytosolic delivery might offer a means to evade efflux transporters, such as multidrug-resistance proteins and P-glycoproteins.<sup>[5]</sup> Nanoparticle carriers play a dominant role in this frontier field, at least in part because of their ability to carry a large payload of drug entities protected from extracellular degradation.<sup>[6,7]</sup> However, cells often take up particles through endocytosis, macropinocytosis, or phagocytosis.<sup>[8,9]</sup> Since these processes confine the internalized particles to closed vesicles (endosomes or phagosomes), subsequent fusion of these vesicles with lysosomes often leads to the rapid destruction of therapeutic molecules with little release into the cytosol.<sup>[6]</sup> Thus, the sequestration of drug carriers within endosomes following endocytosis is one of the most critical bottlenecks for cytosolic drug delivery.<sup>[10,11]</sup> Recent studies in this research area have focused on increasing the ability of nanocarriers to escape endolysosomes through controlled lysosomal destabilization (e.g., triggered by the lysosomal pH value or enzymes) and the incorporation of membrane-disruptive or fusogenic moieties (e.g., viral peptides).<sup>[12–19]</sup> The engineering of a

nanocarrier that can bypass the endosomal route entirely would open a new avenue for enhanced cytosolic drug delivery.

The scavenger receptor class B type I (SR-BI) mediates the selective transport of cholesterol esters from high-density lipoprotein (HDL)<sup>[20]</sup> to the cytosol of cells, presumably by forming a hydrophobic channel in the cell membrane.<sup>[21]</sup> To exploit this unique non-endocytic uptake mechanism for the direct cytosolic delivery of cancer diagnostics and therapeutics, we created a peptide–phospholipid nanocarrier (denoted as NC). The NC was prepared by three simple steps (Figure 1A): 1) formation of a dry lipid film with 1,2-dimyristoyl-*sn*-glycero-3-phosphocholine (DMPC), cholesterol oleate, and DiR-BOA (1,1'-dioctadecyl-3,3,3',3'-tetramethylindotricarbocyanine iodide bisoleate, a lipid-anchored near-infrared fluorophore to serve as the model drug cargo),<sup>[22]</sup> 2) formation of a lipid emulsion, and 3) titration of the emulsion with an apoA-I-mimetic, amphipathic  $\alpha$ -helical peptide (FAEKFKAEVVDYFAKFWV)<sup>[23]</sup> to produce a core-shell NC that traps DiR-BOA in the core (denoted as DNC; see the Supporting Information for synthetic details).

We hypothesized that the interaction between the self-assembled  $\alpha$ -helical-peptide network and the lipid monolayer would provide the desired structural control over nanoparticle size, monodispersity, and stability, as well as functional control over its cellular uptake mechanism. The DNCs appeared spherical in shape on the basis of transmission electron microscopy (TEM; Figure 1B). However, when the payload was omitted, discoidal particles were observed by TEM, a result consistent with previous studies in which only DMPC was combined with HDL-mimetic peptides.<sup>[24,25]</sup> The shapes observed by TEM are consistent with other reports of discoidal and spherical HDL.<sup>[26,27]</sup>

To distinguish the fate of cargo molecules from that of the nanoparticle components themselves, two additional fluorescein-labeled DNC particles were prepared. In the first, F(lipid)-DNC, a portion of the lipid component was replaced with a fluorescein-labeled lipid (DSPE-PEG-CF). In the second particle, F(peptide)-DNC, some lysine residues on the  $\alpha$ -helical peptide were labeled with fluorescein. All three particles, DNC, F(lipid)-DNC, and F(peptide)-DNC (Figure 1C) were readily synthesized and purified by fast protein liquid chromatography (see Figure 1 in the Supporting Information) and were stable under physiological conditions (37 °C, pH 7.5) for 24 h without DiR-BOA leakage.

The proposed mechanism for direct cytosolic cargo transport by the NC is depicted in Figure 1C. Upon recognition of

[\*] Dr. Z. H. Zhang, Dr. W. G. Cao, H. L. Jin, Dr. M. Yang, L. L. Ding, Dr. J. Chen, Dr. I. Corbin, Dr. G. Zheng  
Department of Medical Biophysics and Ontario Cancer Institute  
University of Toronto, Toronto, Ontario M5G 1L7 (Canada)  
E-mail: gang.zheng@uhnres.utoronto.ca  
Homepage: <http://www.utoronto.ca/zhenglab>

J. F. Lovell, Dr. G. Zheng  
Institute of Biomaterials and Biomedical Engineering  
University of Toronto, Toronto, Ontario M5G 1L7 (Canada)

Dr. Z. H. Zhang, H. L. Jin, Dr. Q. M. Luo  
Britton Chance Center for Biomedical Photonics  
Wuhan National Laboratory for Optoelectronics  
Huazhong University of Science and Technology, Wuhan (China)

Dr. W. G. Cao  
Department of Chemistry, Shanghai University, Shanghai (China)

[\*\*] This study was conducted with the support of the Canadian Institute of Health Research, the Ontario Institute for Cancer Research through funding provided by the Government of Ontario, the Joey and Toby Tanenbaum/Brazilian Ball Chair in Prostate Cancer Research, and the Program for New Century Excellent Talents in University of China (NCET-08-0220, Z.H.Z.). We thank Dr. Monty Krieger of MIT for providing IdIA7 and IdIA(mSR-BI) cell lines.

Supporting information for this article, including full details of the materials and methods used, is available on the WWW under <http://dx.doi.org/10.1002/anie.200903112>.

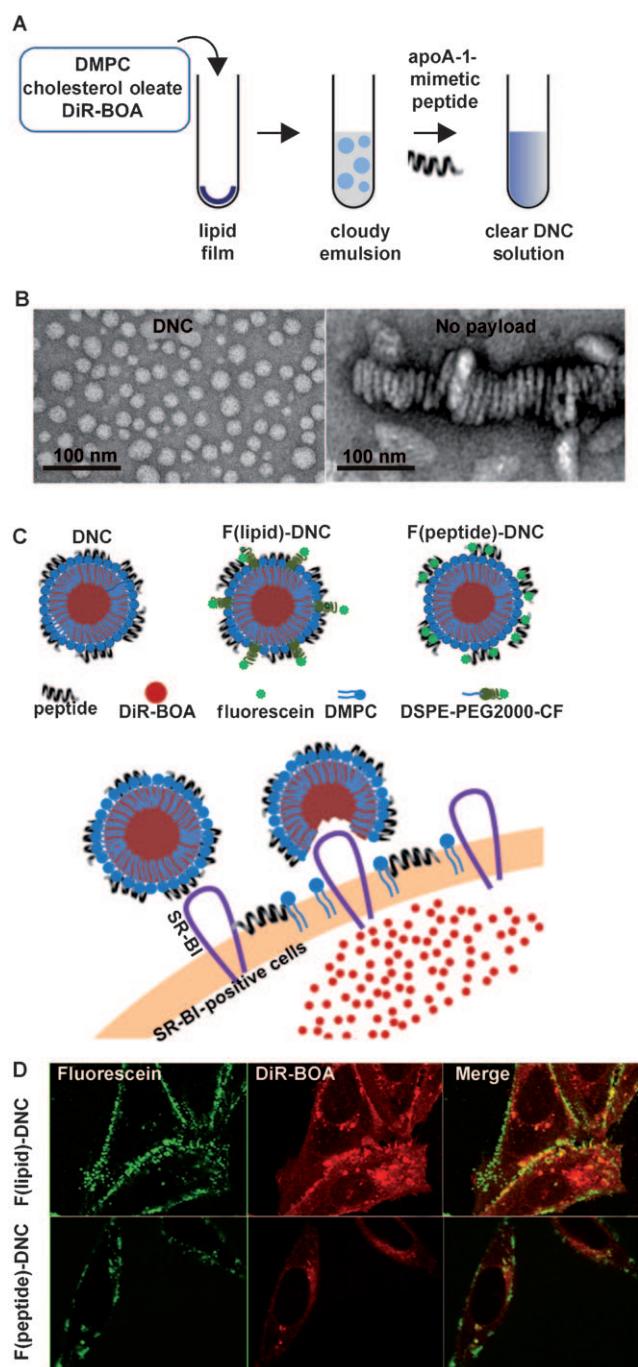


**Figure 1.** Preparation and structure of DNC, and proposed direct cytosolic delivery mechanism. A) DNC synthesis. B) Negatively stained TEM images of DNCs (left) and discoidal particles formed from the peptide and DMPC alone (right). C) Proposed DNC structures and mechanism for the SR-BI-mediated cytosolic delivery of DNC cargo. D) Confocal images of IdIA(mSR-BI) (SR-BI<sup>+</sup>) cells showing the fluorescein-labeled lipid (top) and peptide (bottom) localized on the cell surface and the DiR-BOA cargo in the cytosol. Scale bar is 10  $\mu$ m. A corresponding confocal-stack movie is included in the Supporting Information. apoA-I = apoprotein A-I, DSPE-PEG2000-CF = 1,2-distearoyl-*sn*-glycero-3-phosphoethanolamine-*N*-(poly(ethylene glycol)2000-*N'*-carboxyfluorescein).

DNC by SR-BI, the cell membrane undergoes membrane reorganization, which leads to the cross-membrane transfer of

the DiR-BOA cargo from the NC to cytosolic compartments without internalization of the intact particle. To elucidate this powerful non-endocytotic uptake mechanism, we used LDL-receptor-deficient Chinese hamster ovary cells (IdIA7) stably expressing high levels of murine SR-BI (IdIA(mSR-BI)) as a SR-BI-positive control (SR-BI<sup>+</sup>).<sup>[20]</sup> Confocal imaging studies of F(lipid)-DNC and F(peptide)-DNC incubated with IdIA(mSR-BI) cells for 1 h clearly demonstrated that the cargo DiR-BOA signal was located in the cytosolic compartments, whereas the fluorescein-labeled lipid or peptide was mainly retained on the cell surface (Figure 1D). These results were consistent throughout the cells, as evidenced by 3D movies reconstructed from confocal images at different depths (see movie in the Supporting Information). Thus, cargo transport by the NC is mediated through a non-endocytotic pathway, presumably through SR-BI.

Next, we examined whether non-endocytotic cargo transport by the NC was indeed SR-BI-specific. For this purpose, wild-type IdIA7 cells expressing low levels of endogenous SR-BI were used as a negative control (SR-BI<sup>-</sup>) for comparison with results obtained with the IdIA(mSR-BI) cells (SR-BI<sup>+</sup>). Confocal imaging studies (Figure 2A; see also Figure 2B in the Supporting Information) showed strong uptake of DNC in IdIA(mSR-BI) cells but not in IdIA7 cells, and its uptake in IdIA(mSR-BI) cells was clearly inhibited by the presence of HDL (the native SR-BI ligand). The SR-BI-targeting specificity of DNC was further quantified by flow cytometry studies. A 55-fold difference ( $n = 5$ ,  $P < 0.001$ ) in DiR-BOA uptake was observed between IdIA(mSR-BI) and IdIA7 cells (Figure 2B). Fluorescence of the DiR-BOA cargo in IdIA(mSR-BI) cells was completely blocked by native HDL inhibition ( $\approx 98\%$ ,  $n = 5$ ,  $P < 0.001$ ). These results suggest that non-endocytotic cargo transport by NC is mediated by SR-BI.

We then evaluated the utility of the NC for cytosolic delivery in cancer cells. A number of human cancers (e.g., breast cancer) are known to overexpress SR-BI receptors. On the basis of western blot and confocal imaging data (see Figures 2A and 2B in the Supporting Information), we selected the human epidermoid carcinoma KB cell line (KB). We also selected a human metastatic breast cancer cell line (MT-1) as an SR-BI<sup>+</sup> control, a human fibrosarcoma cell line (HT1080) as an SR-BI<sup>-</sup> control, and the IdIA(mSR-BI) cell line as an SR-BI<sup>+</sup> reference. Consistent with the pattern of direct cytosolic delivery, significant DiR-BOA uptake in all SR-BI<sup>+</sup> cells was observed, and the DiR-BOA signals were not colocalized with those of LysoTracker (Figure 3). No DiR-BOA uptake was observed in the SR-BI<sup>-</sup> HT1080 cancer cells. Thus, the nonlysosomal localization of DiR-BOA (core cargo) combined with the cell-surface retention of both the lipid and the peptide (Figure 1D) clearly point to a mechanism involving SR-BI-mediated direct cytosolic cargo transport.

To test the potential utility of the NC for SR-BI-mediated cargo transport *in vivo*, a double tumor-bearing mouse model was introduced with KB (SR-BI<sup>+</sup>) on the left flank and HT1080 (SR-BI<sup>-</sup>) on the right flank. Whole-body optical images clearly showed the preferential accumulation of DNC in the SR-BI<sup>+</sup> tumor versus the SR-BI<sup>-</sup> tumor (Figure 2C): a 3.8-fold difference was calculated by *ex vivo* measurement of

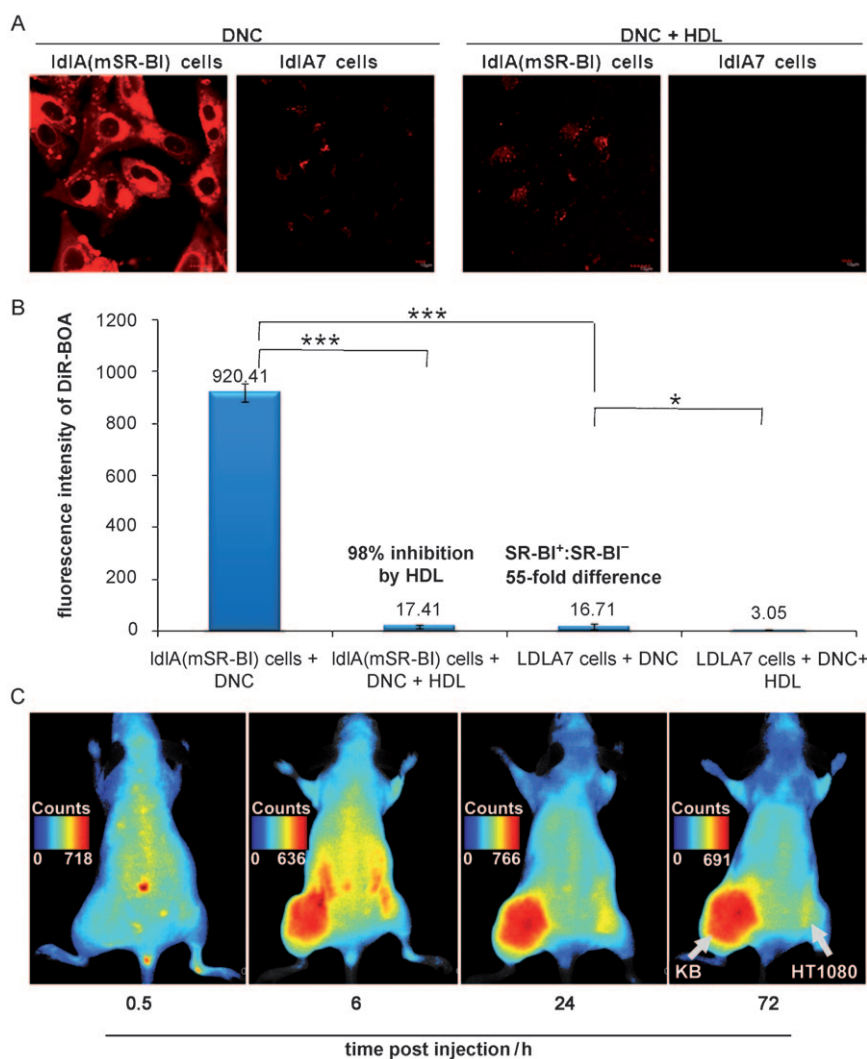


**Figure 2.** Validation of the SR-BI specificity of DNC. A) Confocal imaging and B) flow cytometry studies on IdIA(mSR-BI) (SR-BI<sup>+</sup>) cells and IdIA7 (SR-BI<sup>-</sup>) cells demonstrated the SR-BI targeting of DNC. Mean values  $\pm$  standard deviation (SD),  $n=5$ ;  $P$  values were calculated on the basis of a nonpaired two-tailed Student  $t$  test (\* $P < 0.05$ , \*\* $P < 0.01$ , \*\*\* $P < 0.001$ ). C) Monitoring of the targeting accumulation of DNC in vivo by using a whole-body optical imaging system at 0.5, 6, 24, and 72 h postinjection (representative of three experiments). A color-coded scale of the fluorescence counts is shown.

harvested-tumor fluorescence normalized to the mass of the excised tumors. Biodistribution data indicated that DiR-BOA accumulation was high in the tumor and surpassed only by accumulation in the liver (see Figure 3 in the Supporting Information). The above results reveal the in vivo utility of the NC for enhanced cytosolic drug delivery. Caution must be exercised in interpreting the presented xenograft data, as xenograft growth rates, tumor microenvironments, and stroma characteristics may have been different, and these factors would affect the amount of DiR-BOA uptake.

To demonstrate that the NC system can be extended beyond DiR-BOA, we synthesized Fluo-BOA,<sup>[28]</sup> which consists of a two oleoyl groups conjugated to a hydrophilic fluorescein dye (Figure 4A). Fluo-BOA was readily loaded

into the NCs by the procedure used for DiR-BOA. Like DNC, the Fluo-BOA NC was taken up selectively by cells expressing the SR-BI receptor (Figure 4B). Z stacks in confocal microscopy indicated that the NC cargo was delivered to the cytosol of cells (see arrows in Figure 4C). This result was further confirmed by a subcellular fractionation assay showing the preferential accumulation of the fluorescent cargo in the cytosol (63% of the total intracellular signal) versus nuclei (12%) and other subcellular organelles, including lysosomes (25%; Figure 4D). Finally, when live cells were incubated with the lipophilic fluorescent tracer 1,1'-dioctadecyl-3,3,3',3'-tetramethylindocarbocyanine perchlorate (DiI), a distinct difference was observed in the localization of DiI and Fluo-BOA: whereas DiI was found primarily on the plasma membrane, Fluo-BOA was localized in the cytosol of the cell (Figure 4E). These data, taken together, strongly point to the delivery of the NC cargo to the cytosol of the cell.

The central hypothesis of this study was that a simple and robust peptide-phospholipid nanocarrier could be developed to mimic the HDL/SR-BI-mediated cholesterol-transport mechanism and thus bypass the formidable threat posed by the endosomal trapping of drug carriers. Our results strongly support this hypothesis. The NC system has several advantages in addition to that of direct cytosolic delivery. First, the biomimetic nature of the peptide-phospholipid assembly offers precise size control. The NC is highly monodisperse with a distinct core-shell structure of 10–30 nm; thus, it is able to diffuse freely through interstitial spacing (< 40 nm):<sup>[29]</sup> a key advantage for the enhancement of both accumulation and internalization in tumors.<sup>[30–32]</sup> Second, all structural components of the NC, including the apoA-1-mimetic peptide,<sup>[23]</sup> the phospholipid,<sup>[33]</sup> and cholesteryl oleate, are highly biocompatible. For example, several apoA-1-mimetic peptides are in advanced clinical trials for high-risk cardiovascular patients.<sup>[23,34]</sup> Evidence of the biocompatibility of the NC was also obtained from an in vitro MTT assay and a preliminary in vivo acute toxicity test (data not shown; MTT = 3-(4,5-dimethylthiazol-2-yl)-2,5-diphenyltetrazolium bromide). Third, the biomimetic surface properties of the NC system are responsible for its long circulation half-life (ca. 15 h; see Figure 4 in the Supporting Information), which is similar to that of HDL<sup>[35]</sup> and comparable to

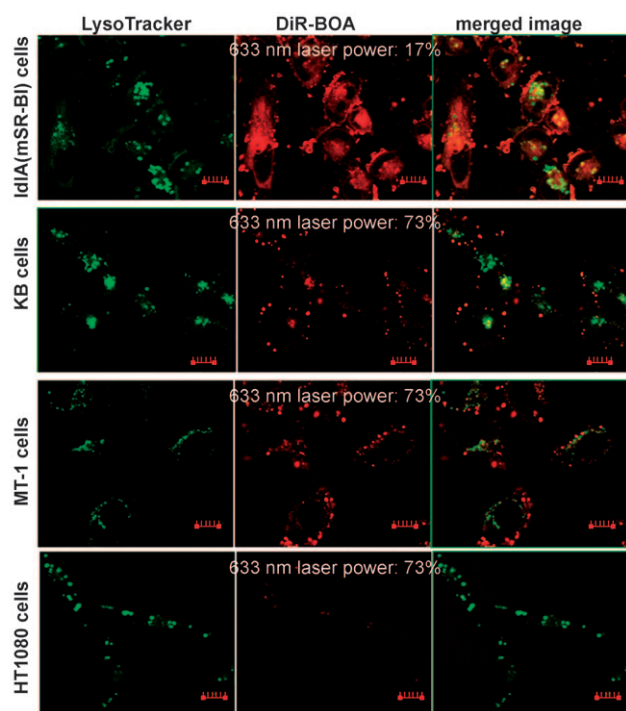


**Figure 3.** Validation of the SR-BI-mediated, non-endocytotic cargo-delivery mechanism in cancer cells by confocal imaging studies. Top: IdIA(mSR-BI) cells, SR-BI<sup>+</sup> reference cells; middle two rows: SR-BI<sup>+</sup> KB and MT-1 cancer cells; bottom: SR-BI<sup>-</sup> HT1080 cancer cells. The fluorescent images from left to right are of the cells with LysoTracker, the cells with DiR-BOA, and a merged fluorescent image showing the localization of LysoTracker and DiR-BOA simultaneously. Scale bar is 10 µm.

that of some of the best engineered (PEGylated) long-circulating liposomes to date.<sup>[36]</sup> (The clearance kinetics were based on the DiR-BOA fluorescence signal, which may have been partially redistributed from DNC to serum proteins over time.) Finally, the NC system is also versatile, with the capability to carry a range of diagnostic and therapeutic cargo molecules. DiR and fluorescein, two small-molecule fluorophores of different hydrophobicity, were amenable to bis-oleoyl-based NC incorporation. Other molecules, such as paclitaxel, have proven amenable to bisoleoyl modification and NC loading (data not shown). Although small hydrophobic and hydrophilic molecules can be loaded upon modification to render them suitably hydrophobic, there are probably limitations even if molecules are conjugated through bisoleoyl to the carrier system. For example, it is likely that oligonucleotides cannot be loaded into the NC core owing to their highly charged nature. The system described herein is for the delivery of hydrophobic molecules. Further studies are required for a better understanding of exactly what types of cargo can be loaded into and delivered with the NC. However, our initial explorations have demonstrated the potential clinical utility of this novel method for cytosolic drug delivery.

In summary, we created a novel biomimetic NC system with biocompatible components and peptide-mediated struc-

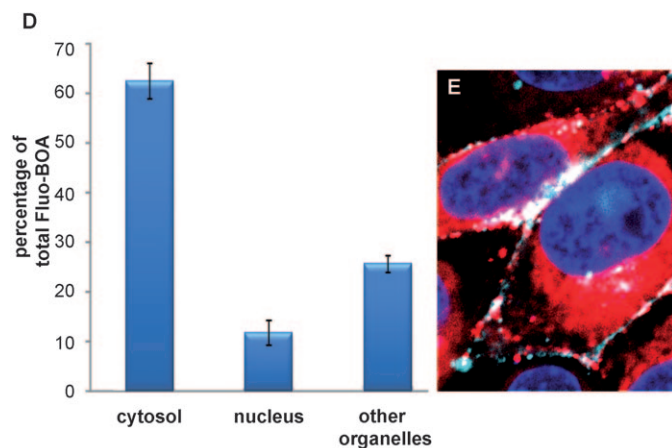
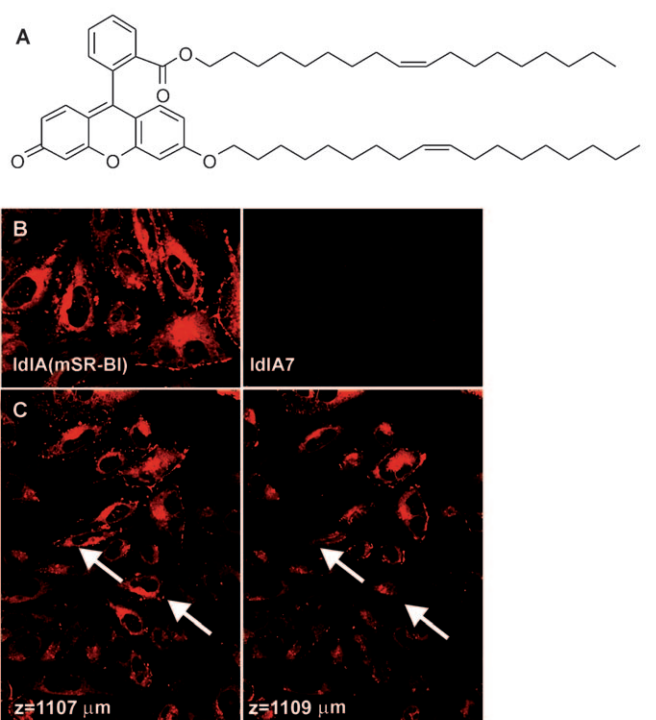


**Figure 4.** Cytosolic delivery of Fluo-BOA. A) Structure of Fluo-BOA. B) Confocal microscopy of Fluo-BOA loaded into NCs after incubation with cells that express SR-BI (IdIA(mSR-BI)) or cells that do not express SR-BI (IdIA7). C) Confocal z stacks showing the cytosolic localization of Fluo-BOA after NC delivery to SR-BI<sup>+</sup> cells. D) Uptake of Fluo-BOA-NC in different (SR-BI-expressing) MT-1 subcellular fractions, as determined by using the Focus Subcell kit (mean  $\pm$  SD,  $n=3$ ). E) Cytosolic localization of NC-delivered Fluo-BOA in IdIA(mSR-BI) cells. Cell nuclei were labeled with a Hoescht stain (blue); cell membranes were labeled with Dil (cyan) after incubation of the cells with Fluo-BOA-NC (red) for 2 h.

tural and functional control. More importantly, by using a near-infrared dye (DiR-BOA) as a model NC cargo together with various fluorescence imaging techniques, we confirmed the feasibility of using an NC to directly transport functional cargo to the cytosol of cancer cells without the involvement of endolysosomal trafficking. The direct transport mechanism of

our NC system is a key advantage for the delivery of intracellular active cancer agents.

Received: June 9, 2009

Revised: September 29, 2009

Published online: October 28, 2009

**Keywords:** biomimetic structures · cytosol · drug delivery · nanocarriers · peptides

- 
- [1] T. M. Allen, P. R. Cullis, *Science* **2004**, *303*, 1818.
- [2] W. R. Sanhai, J. H. Sakamoto, R. Canady, M. Ferrari, *Nat. Nanotechnol.* **2008**, *3*, 242.
- [3] K. A. Whitehead, R. Langer, D. G. Anderson, *Nat. Rev. Drug Discovery* **2009**, *8*, 129.
- [4] D. Schweichel, J. Steitz, D. Tormo, E. Gaffal, A. Ferrer, S. Buchs, P. Speuser, A. Limmer, T. Tuting, *J. Gene Med.* **2006**, *8*, 1243.
- [5] J. Panyam, V. Labhasetwar, *Curr. Drug Delivery* **2004**, *1*, 235.
- [6] M. E. Davis, Z. G. Chen, D. M. Shin, *Nat. Rev. Drug Discovery* **2008**, *7*, 771.
- [7] L. Zhang, F. X. Gu, J. M. Chan, A. Z. Wang, R. S. Langer, O. C. Farokhzad, *Clin. Pharmacol. Ther.* **2008**, *83*, 761.
- [8] G. W. Gould, J. Lippincott-Schwartz, *Nat. Rev. Mol. Cell Biol.* **2009**, *10*, 287.
- [9] J. Mercer, A. Helenius, *Nat. Cell Biol.* **2009**, *11*, 510.
- [10] V. P. Torchilin, *Pharm. Res.* **2007**, *24*, 1.
- [11] V. P. Torchilin, *Nat. Rev. Drug Discovery* **2005**, *4*, 145.
- [12] R. Juliano, M. R. Alam, V. Dixit, H. Kang, *Nucleic Acids Res.* **2008**, *36*, 4158.
- [13] M. V. Yezhelyev, L. Qi, R. M. O'Regan, S. Nie, X. Gao, *J. Am. Chem. Soc.* **2008**, *130*, 9006.
- [14] H. Devalapally, D. Shenoy, S. Little, R. Langer, M. Amiji, *Cancer Chemother. Pharmacol.* **2007**, *59*, 477.
- [15] Y. Hu, T. Litwin, A. R. Nagaraja, B. Kwong, J. Katz, N. Watson, D. J. Irvine, *Nano Lett.* **2007**, *7*, 3056.
- [16] B. Y. Kim, W. Jiang, J. Oreopoulos, C. M. Yip, J. T. Rutka, W. C. Chan, *Nano Lett.* **2008**, *8*, 3887.
- [17] K. C. Partlow, G. M. Lanza, S. A. Wickline, *Biomaterials* **2008**, *29*, 3367.
- [18] A. M. Derfus, A. A. Chen, D. H. Min, E. Ruoslahti, S. N. Bhatia, *Bioconjugate Chem.* **2007**, *18*, 1391.
- [19] J. K. Vasir, V. Labhasetwar, *Adv. Drug Delivery Rev.* **2007**, *59*, 718.
- [20] S. Acton, A. Rigotti, K. T. Landschulz, S. Xu, H. H. Hobbs, M. Krieger, *Science* **1996**, *271*, 518.
- [21] W. V. Rodriguez, S. T. Thuahnai, R. E. Temel, S. Lund-Katz, M. C. Phillips, D. L. Williams, *J. Biol. Chem.* **1999**, *274*, 20344.
- [22] I. R. Corbin, J. Chen, W. Cao, H. Li, S. Lund-Katz, G. Zheng, *J. Biomed. Nanotechnol.* **2007**, *3*, 367.
- [23] M. Navab, G. M. Anantharamaiah, S. T. Reddy, A. M. Fogelman, *Nat. Clin. Pract. Cardiovasc. Med.* **2006**, *3*, 540.
- [24] A. von Eckardstein, G. Castro, I. Wybranska, N. Theret, P. Duchateau, N. Duverger, J. C. Fruchart, G. Ailhaud, G. Assmann, *J. Biol. Chem.* **1993**, *268*, 2616.
- [25] V. K. Mishra, M. N. Palgunachari, R. Krishna, J. Glushka, J. P. Segrest, G. M. Anantharamaiah, *J. Biol. Chem.* **2008**, *283*, 34393.
- [26] D. L. Sparks, W. S. Davidson, S. Lund-Katz, M. C. Phillips, *J. Biol. Chem.* **1995**, *270*, 26910.
- [27] R. A. Silva, R. Huang, J. Morris, J. Fang, E. O. Gracheva, G. Ren, A. Kontush, W. G. Jerome, K. A. Rye, W. S. Davidson, *Proc. Natl. Acad. Sci. USA* **2008**, *105*, 12176.
- [28] M. Krieger, L. C. Smith, R. G. Anderson, J. L. Goldstein, Y. J. Kao, H. J. Pownall, A. M. Gotto, Jr., M. S. Brown, *J. Supramol. Struct.* **1979**, *10*, 467.
- [29] A. Pluen, Y. Boucher, S. Ramanujan, T. D. McKee, T. Gohongi, E. di Tomaso, E. B. Brown, Y. Izumi, R. B. Campbell, D. A. Berk, R. K. Jain, *Proc. Natl. Acad. Sci. USA* **2001**, *98*, 4628.
- [30] N. Tang, G. Du, N. Wang, C. Liu, H. Hang, W. Liang, *J. Natl. Cancer Inst.* **2007**, *99*, 1004.
- [31] M. R. Dreher, W. Liu, C. R. Michelich, M. W. Dewhirst, F. Yuan, A. Chilkoti, *J. Natl. Cancer Inst.* **2006**, *98*, 335.
- [32] S. D. Perrault, C. Walkey, T. Jennings, H. C. Fischer, W. C. W. Chan, *Nano Lett.* **2009**, *9*, 1909.
- [33] M. Navab, S. Hama, G. Hough, A. M. Fogelman, *Circulation* **2003**, *108*, 1735.
- [34] D. Duffy, D. J. Rader, *Curr. Opin. Cardiol.* **2005**, *20*, 301.
- [35] S. Eisenberg, H. G. Windmueller, R. I. Levy, *J. Lipid Res.* **1973**, *14*, 446.
- [36] S. M. Moghimi, A. C. Hunter, J. C. Murray, *Pharmacol. Rev.* **2001**, *53*, 283.
-